

Supporting Information for

ORIGINAL ARTICLE

pH-Sensitive and bubble-generating mesoporous silica-based nanoparticles for enhanced tumor combination therapy

Zhiming Zhang[†], Chenlu Huang[†], Li Zhang, Qing Guo, Yu Qin, Fan Fan, Boxuan Li, Bao Xiao, Dunwan Zhu^{*}, Linhua Zhang^{*}

Tianjin Key Laboratory of Biomedical Materials, Key Laboratory of Biomaterials and Nanotechnology for Cancer Immunotherapy, Institute of Biomedical Engineering, Chinese Academy of Medical Sciences & Peking Union Medical College, Tianjin 300192, China

Received 16 April 2020; received in revised form 28 June 2020; accepted 24 July 2020

^{*}Corresponding authors.

E-mail addresses: zhudunwan@bme.pumc.edu.cn (Dunwan Zhu), zhanglinhua@bme.pumc.edu.cn (Linhua Zhang).

[†]These authors made equal contributions to this work.

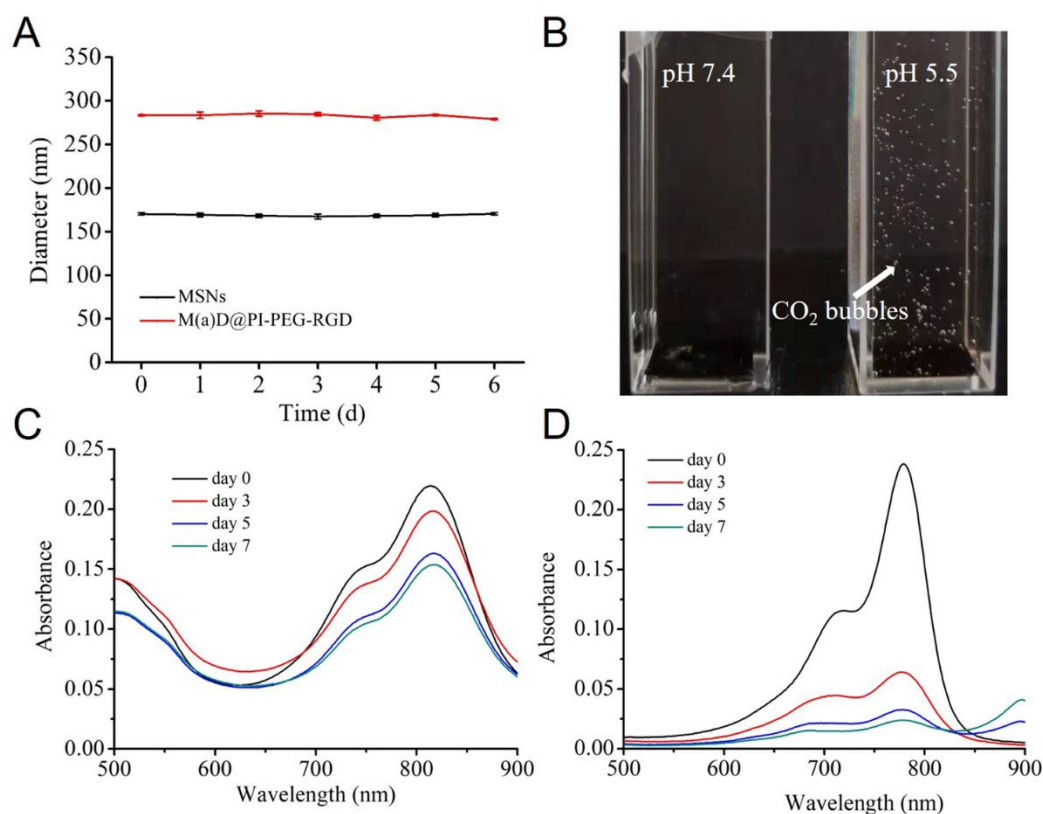


Figure S1 (A) Size stability of nanoparticles (MSNs and M(a)D@PI-PEG-RGD). All data represented as mean \pm SD ($n = 3$). (B) Image of M(a)D@PI-PEG-RGD nanoparticles added into PBS (pH7.4, 5.5). (C) and (D) UV-Vis spectra of

M(a)D@PI-PEG-RGD and ICG from dispersed in distilled water to 7 days.

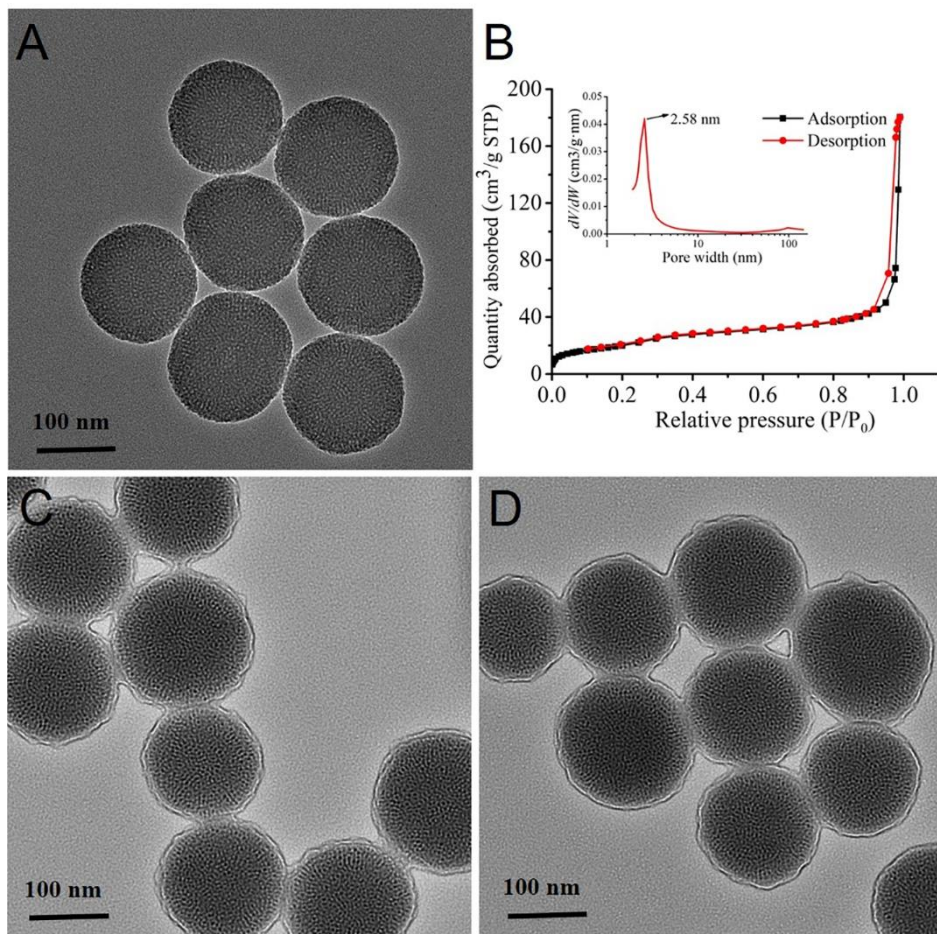


Figure S2 Morphological characterization of nanoparticles. (A) TEM image of MSNs. (B) N₂ adsorption-desorption isotherms and pore size distribution from BJH adsorption of MSNs. (C) TEM image of M(a)D@P; (D) TEM images of M(a)D@PI-PEG.

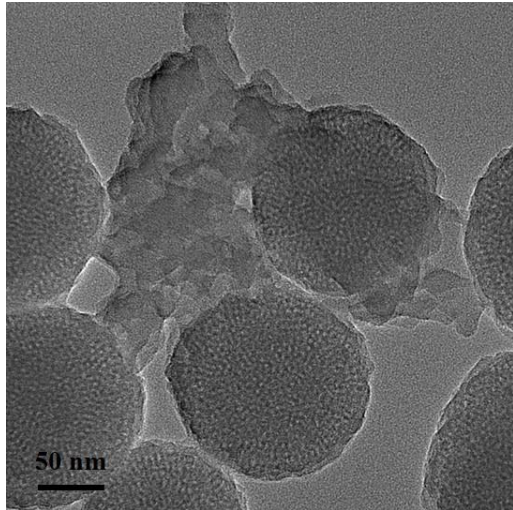


Figure S3 TEM image of M(a)D@PI-PEG treated with laser irradiation (808 nm, 1 W/cm², 5 min).

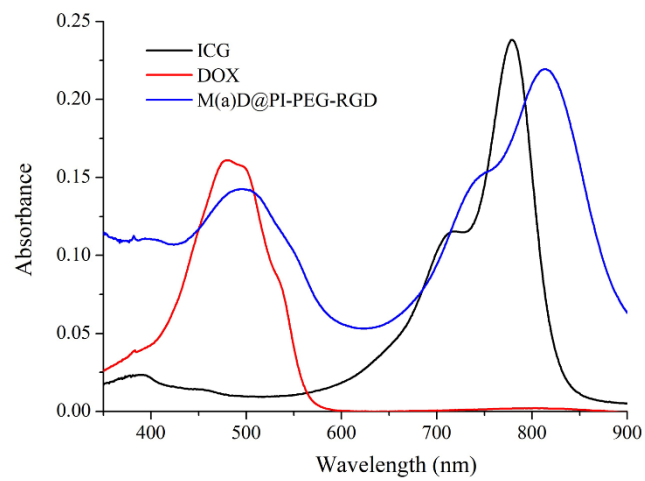


Figure S4 UV-Vis spectra of M(a)D@PI-PEG-RGD, DOX and ICG.

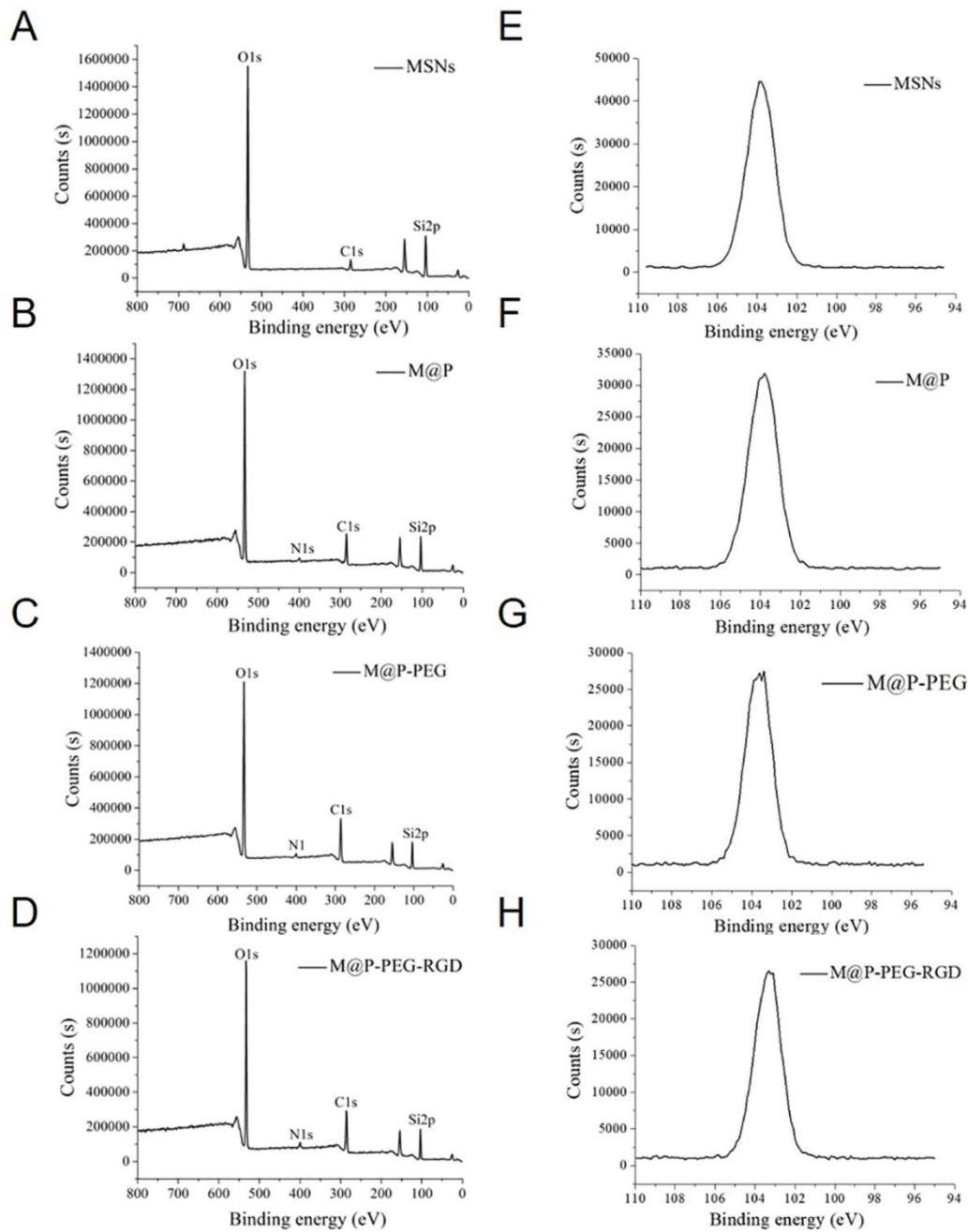


Figure S5 XPS spectra of MSNs, M@P, M@P-PEG and M@P-PEG-RGD. (A)–(D) Wide scan; (E) and (H) Narrow scan for Si2p peaks.

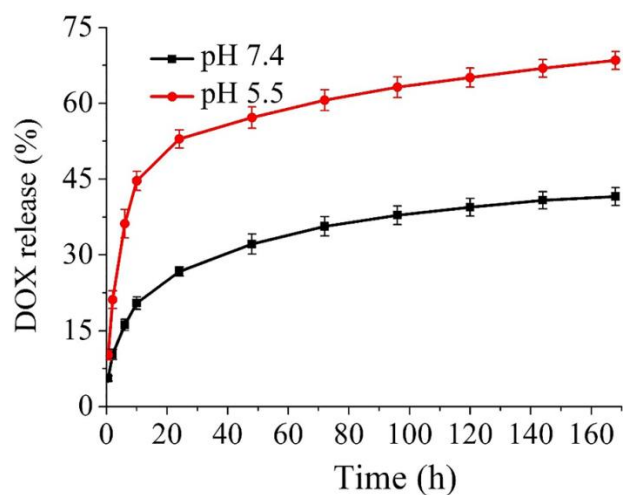


Figure S6 DOX release curves of M(a). The data were shown as mean \pm SD ($n=3$).

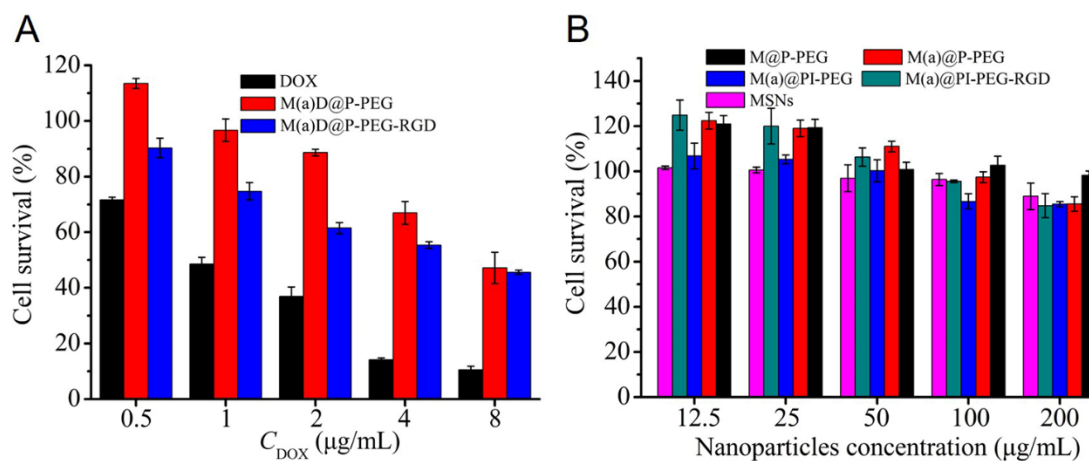


Figure S7 The cytotoxicity of different formulations. (A) Survival of CT26 treated with various formulations at different DOX concentrations for 48 h. (B) Survival of CT26 treated with various formulations at concentrations for 72 h. All data represented as mean \pm SD ($n = 3$).

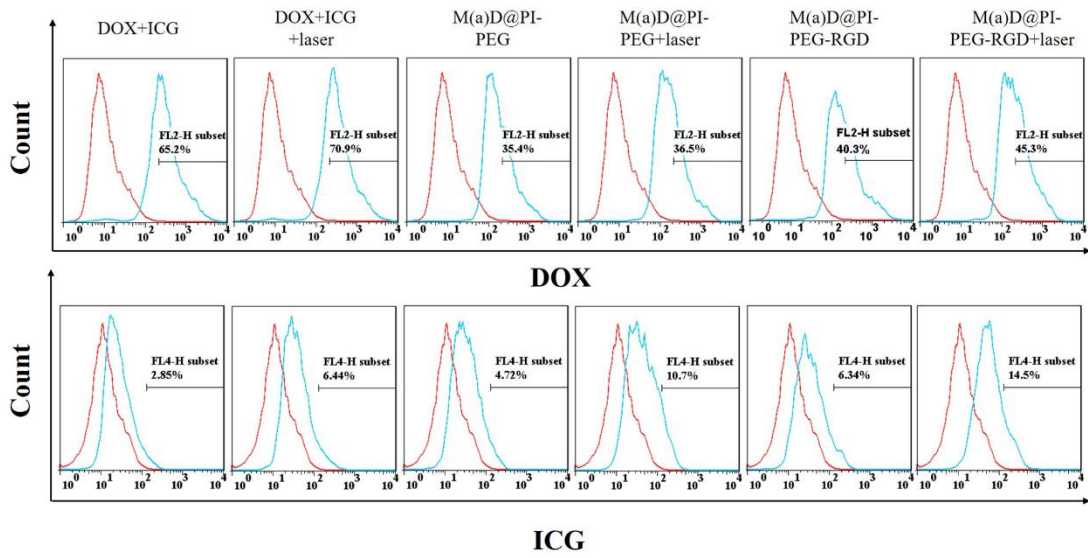


Figure S8 Flow cytometry detection of DOX and ICG in CT26 cells incubated with different formulations. Laser: 808 nm, 1 W/cm², 5 min.

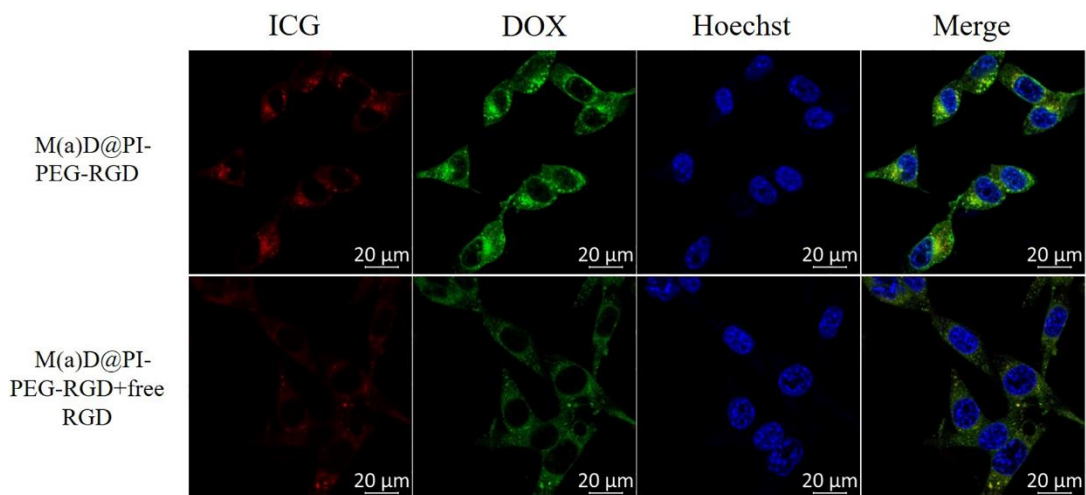


Figure S9 CLSM images of CT26 cells treated with different formulations (with the same DOX equivalent concentration, 8 μg/mL) for competitive binding experiments.

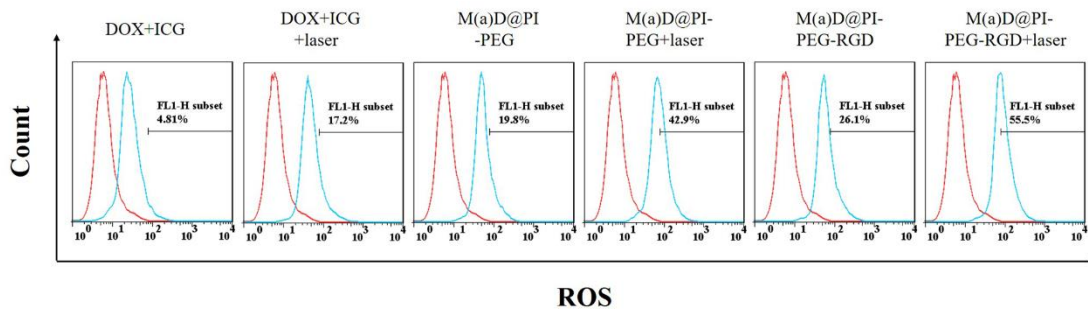


Figure S10 Flow cytometry of CT26 cells incubated with different formulations for ROS detection for three times. Laser: 808 nm, 1 W/cm², 5 min.

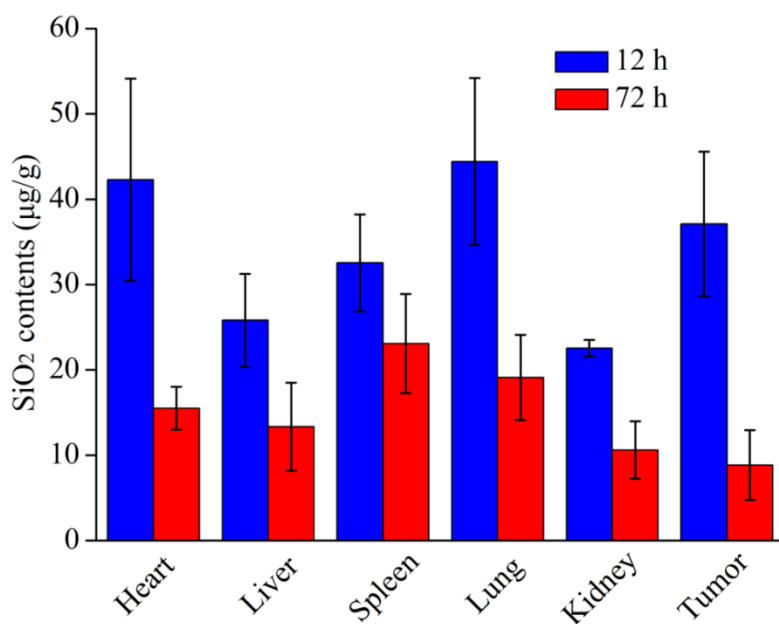


Figure S11 Quantitative analysis of the distribution of M(a)D@PI-PEG-RGD in organs by ICP-MS. The data represented as mean \pm SD ($n = 3$).

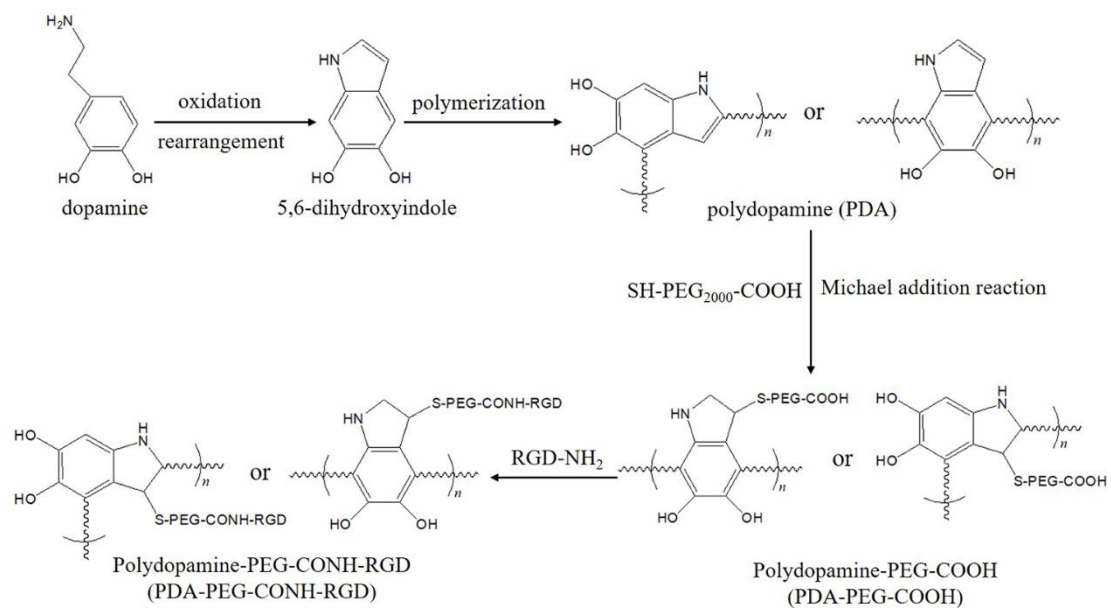


Figure S12 The synthetic route of RGD-PEG₂₀₀₀-conjugated PDA layer.